

Dispersion Effects in Stabilizing Organometallic Compounds: The Tetra-1-norbornyl Derivatives of the First Row Transition Metals as Exceptional Examples

Huidong Li,^{a,b*} Yucheng Hu,^a Di Wan,^a Ze Zhang,^a Qunchao Fan,^a R. Bruce King^{b,*}, and Henry F. Schaefer III^b

^a*Research Center for Advanced Computation, School of Science, Xihua University, Chengdu, China 610039*

^b*Center for Computational Quantum Chemistry, University of Georgia, Athens, Georgia, USA 30602*

Abstract.

In 1972 Bower and Tennett first synthesized a series of tetra-1-norbornyl derivatives, $(\text{nor})_4\text{M}$, of the first-row transition metals from titanium to cobalt. These were found to be exceptionally stable for homoleptic metal alkyls containing only metal-carbon σ -bonds. The theoretical energies for the dissociation of 1-norbornyl ligands from these unusually high oxidation state organometallics through the reactions $(\text{nor})_4\text{M} \rightarrow (\text{nor})_3\text{M} + \text{nor}\cdot$ and $(\text{nor})_4\text{M} \rightarrow (\text{nor})_2\text{M} + \text{nor-nor}$ indicate that dispersion effects play an important role in determining their exceptional stability. Thus all of the $(\text{nor})_4\text{M}$ ($\text{M} = \text{Ti}$ to Cu) derivatives are viable with respect to 1-norbornyl radical dissociation when the London dispersion effect is considered. However, $(\text{nor})_4\text{Cu}$ becomes disfavored if the dispersion correction is ignored. Thus the stability of the $(\text{nor})_4\text{M}$ molecules is seen to arise from the favorable combination of steric and dispersion force effects of the four 1-norbornyl groups tetrahedrally disposed around the metal atom and maximizing the dispersion attraction between them in a spherical hydrocarbon structures with a central metal atom. The tri-1-norbornyl derivatives $(\text{nor})_3\text{M}$ appear be disfavored with respect to disproportionation into $(\text{nor})_4\text{M} + (\text{nor})_2\text{M}$. This is consistent with the experimental syntheses of the $(\text{nor})_4\text{M}$ ($\text{M} = \text{Cr}$ to Co) derivatives with the metal in the +4 oxidation by reactions with 1-norbornyllithium with metal halides in the +2 or +3 metal oxidation states. Both the OPBE method and the BPW91 method predict high spin states for the d^2 and d^3 complexes $(\text{nor})_4\text{Cr}$ and $(\text{nor})_4\text{Mn}$ but low spin states for $(\text{nor})_4\text{Fe}$ and $(\text{nor})_4\text{Co}$, consistent with experiment.

e-mail addresses: huidongli@mail.xhu.edu.cn (Huidong Li); rbking@chem.uga.edu (R. Bruce King)

1. Introduction

Most homoleptic transition metal alkyls of the general type ML_n are not viable species since the central metal atoms lack the ancillary ligands such as carbonyl, cyclopentadienyl, etc., to attain the favored 18-electron configuration.^{1,2,3} In addition, metal alkyls with CH_2 -hydrogen atoms on the alkyl group are generally disfavored with respect to CH_2 -hydrogen migration to the metal atom, thereby eliminating an olefin to give the corresponding metal hydride derivative. The 1-norbornyl group (nor), although containing six CH_2 -hydrogen atoms, is not subject to such CH_2 -hydrogen migration since the resulting olefin, 1-norbornene, is highly strained because one of the sp^2 carbons of the $\text{C}=\text{C}$ double bond would be located at a bridgehead according to Bredt's rule (Figure 1).⁴

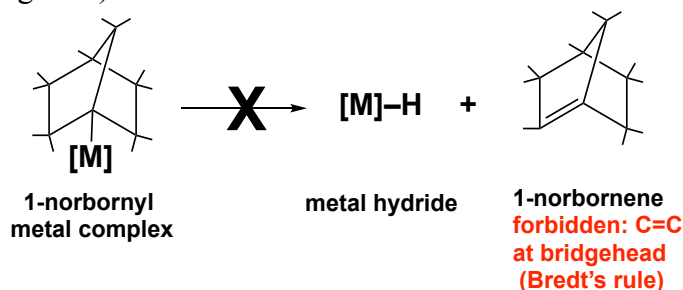


Figure 1. CH_2 -Hydrogen migration from a 1-norbornyl metal complex to the metal atom is unfavorable by Bredt's rule since it gives the highly strained olefin 1-norbornene having a $\text{C}=\text{C}$ double bond at a bridgehead carbon atom.

Bower and Tennett in 1972⁵ were the first to exploit this characteristic of the 1-norbornyl ligand to synthesize isolable homoleptic transition metal alkyls by reactions of 1-norbornyllithium with metal halides. Even considering the possibility of stabilizing transition metal-carbon bonds by excluding CH_2 -hydrogen elimination, the effects of the special properties of the 1-norbornyl ligand in stabilizing otherwise unusual homoleptic alkyls were found to be truly exceptional. Thus, isolable tetra-1-norbornylmetal derivatives $(\text{nor})_4\text{M}$ ($\text{nor} = 1\text{-norbornyl}$) were synthesized for all of the first row transition metals from titanium to cobalt. This included the first row transition metals from chromium to nickel for which the implied +4 metal oxidation state of their $(\text{nor})_4\text{M}$ derivatives would be clearly considered as unusual (Figure 2). Most striking among these transition metal tetraalkyls was the chromium derivative $(\text{nor})_4\text{Cr}$, which was found to be not only air stable, but also thermally stable up to 250°C in the absence of air, despite the fact that the +4 oxidation state is an unusual one for chromium. Later, after numerous unsuccessful attempts,⁶ the molybdenum analogue $(\text{nor})_4\text{Mo}$ was synthesized from $\text{MoCl}_3(\text{thf})_3$ and 1-norbornyl lithium and found to be air-stable and sublimable in vacuum at 130°C without decomposition.⁷ X-ray crystallography of the representative $(\text{nor})_4\text{M}$ ($\text{M} = \text{Fe},^8 \text{Co}^9$) derivatives clearly indicates tetrahedral coordination of the central metal atom by

forming four metal-carbon σ -bonds although further elucidation of structural details was complicated by disorder. Nevertheless, the $(\text{nor})_4\text{M}$ molecules clearly can be viewed as spherical hydrocarbon structures with a transition metal in the center.

The exceptional stability of the $(\text{nor})_4\text{M}$ derivatives of the first row transition metals might be attributed to the steric hindrance of the 1-norbornyl group combined with the disfavored migration of the σ -hydrogen atoms of the 1-norbornyl group. This suggests that 1-norbornyl transition metal chemistry might be a very rich field. However, only a limited number of other types of 1-norbornyl transition metal complexes are known. These include the stable $(\text{nor})_3\text{NiBr}$, synthesized by Dmitrov and Linden,¹⁰ in which the exceptionally high nickel(IV) oxidation state coexists with the potentially oxidizable bromide ligand. In addition the unstable cyclopentadienyl $(\text{C}_5\text{H}_5)\text{Ni}(\text{nor})$ has been generated at low temperatures from $(\text{C}_5\text{H}_5)_2\text{Ni}$ and 1-norbornyllithium.¹¹

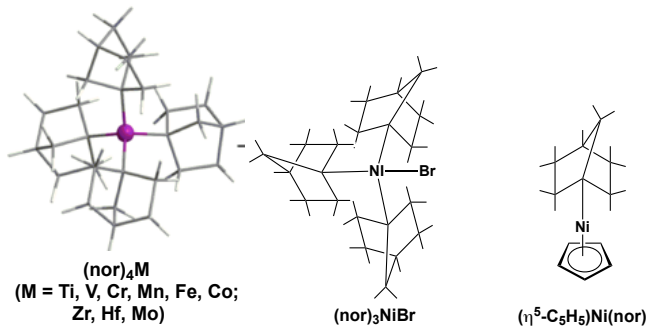


Figure 2. Experimentally known 1-norbornyl transition metal complexes.

The exceptional stability of the $(\text{nor})_4\text{M}$ complexes contrasted with the limited chemistry of other 1-norbornylmetal derivatives suggests the involvement of factors besides the special properties of the 1-norbornyl group. Previous studies have shown that London dispersion can stabilize some types of metal complexes.^{12,13,14} In this connection we have explored the contribution of London dispersion involving the attractive part of the van der Waals potential to the stability of the first row transition metal $(\text{nor})_4\text{M}$ derivatives. This dispersion effect is usually described by instantaneous dipoles induced between two different moieties of molecules or two atoms. The strength of London dispersion forces decreases significantly with increasing distances between atoms or molecular moieties. Thus, for atoms or small molecules this kind of dispersion is usually so small that it can be ignored. However, London dispersion effects can be additive over the entire volume of bulk materials or large molecules thereby becoming significant in solid materials, large molecules, or different moieties within molecules bearing large sterically demanding hydrocarbon ligands.^{15,16,17} In the last systems London dispersion forces can be significant between C–H bonds

which are forced to close separations by the steric demands of bulky hydrocarbon ligands. In this connection the thermochemical properties of molecules, the catalytic characteristics of large molecules, the stabilities of branched alkanes, and the $\square\text{-}\square$ or $\square\text{-}\square$ attractions between hydrocarbon systems could be significantly modified by London dispersion effects.¹⁸ The recent synthesis of $\text{Fe}(\text{cyclohexyl})_4$ by Fürstner and coworkers¹⁹ having a structure with 24 $\square\text{-hydrogen}$ atoms demonstrates that stabilization by London dispersion effects can even override decomposition of homoleptic metal alkyls by $\square\text{-hydrogen}$ elimination.

The geometry of the $(\text{nor})_4\text{M}$ complexes as spherical hydrocarbon structures built from bulky rigid 1-norbornyl ligands with a metal atom in the center makes them exceptional candidates for organometallic compounds stabilized by London dispersion forces. Modern density functional methods provide a way of evaluating the magnitude of such dispersion forces. In this connection such methods have been used for study of 1-norbornyl derivatives of the late transition metals iron, cobalt, and nickel in order to quantify significant London dispersion effects in contributing ~ 40 kcal/mol towards the stability of the iron and cobalt $(\text{nor})_4\text{M}$ derivatives.²⁰ Our study, reported here, provides a more general exploration of the role of London dispersion effects in determining the stabilities of the complete range of $(\text{nor})_4\text{M}$ derivatives of the first row transition metals from titanium to copper. These studies include the thermodynamics of dissociation of 1-norbornyl ligands from the $(\text{nor})_4\text{M}$ derivatives either as 1-norbornyl radicals ($\text{nor}\cdot$) or as bis(1-norbornyl) dimers (nor-nor).

2.Theoretical Methods

Double- \square plus polarization (DZP) basis sets were used in this research. For carbon one set of pure spherical harmonic d functions with orbital exponent $\square_d(\text{C}) = 0.75$ is added to the standard Huzinaga-Dunning contracted DZ sets. This basis set is designated as $(9s5p1d/4s2p1d)$.^{21,22} For hydrogen, a set of p polarization functions $\square_p(\text{H}) = 0.75$ is added to the Huzinaga-Dunning DZ sets. For the first row transition metals, in our loosely contracted DZP basis sets, the Wachters' primitive sets are used, but augmented by two sets of p functions and one set of d functions, contracted following Hood *et al.*, and designated $(14s11p6d/10s8p3d)$.^{23,24}

The geometries of all structures were fully optimized using both the DZP B3PW91 method^{25,26,27} with the Grimme's D3 dispersion scheme^{28,29} and the DZP OPBE methods.^{30,31,32,33,34} In order to show the effects of dispersion the single point energies without the Grimme's D3 dispersion scheme (DZP B3PW9) were determined at the B3PW91-D3 optimized geometries not considering dispersion effects. All of the computations were carried out with the Gaussian 09 program³⁵ in which the ultrafine grid is the default for evaluating integrals

numerically, while the tight designation is the default for the self-consistent field energy convergence.

3. Results and Discussion

The geometries of tetra-, tri-, and di-norbornyl structures $(\text{nor})_4\text{M}$, $(\text{nor})_3\text{M}$, and $(\text{nor})_2\text{M}$ ($\text{M} = \text{Ti}, \text{V}, \text{Cr}, \text{Mn}, \text{Fe}, \text{Co}, \text{Ni}, \text{Cu}$) were optimized for the lowest energy singlet (or doublet) and triplet (or quartet) electronic states. The energy gaps between the singlet (doublet) and triplet (quartet) $(\text{nor})_4\text{M}$ structures are calculated using the B3PW91/DZP method with the Grimme D3 dispersion scheme. These energy gaps are also calculated using the OPBE/DZP method without considering the dispersion scheme. The results (Tables 1 and 2) show that the two different density functional methods are consistent in predicting the energy gaps of the $(\text{nor})_4\text{M}$ ($\text{M} = \text{Ti}, \text{V}, \text{Cr}, \text{Mn}, \text{Fe}, \text{Co}, \text{Ni}, \text{Cu}$) structures. The singlet-triplet energy gap for $(\text{nor})_4\text{Ti}$ considering dispersion (Table 1) is the largest among all the $(\text{nor})_4\text{M}$ structures, namely 52.1 kcal/mol (B3PW91-D3) or 50.3 kcal/mol (OPBE). The two methods predict that the high spin state structures for $(\text{nor})_4\text{Cr}$ and $(\text{nor})_4\text{Mn}$ are lower in energy than the low spin state structures.

Table 1. Energy differences between the triplet and singlet $(\text{nor})_4\text{M}$ ($\text{M} = \text{Ti}, \text{Cr}, \text{Fe}, \text{Ni}$) structures.

$(\text{nor})_4\text{M}$		Magnetic Moment	ΔE [Triplet–Singlet]	(kcal/mol)
	Exp.	$\mu_{so} = \sqrt{4S(S+1)}$	B3PW91-D3/DZP	OPBE/DZP
Ti	0.00	0.00	52.1	50.3
Cr	2.84	2.83	–42.0	–19.2*
Fe	0.00	0.00	10.1	8.6
Ni	—	0.00	8.0	5.7

*The singlet state is an open shell singlet.

Table 2. Energy differences between the quartet and doublet $(\text{nor})_4\text{M}$ ($\text{M} = \text{V}, \text{Mn}, \text{Co}, \text{Cu}$) structures.

$(\text{nor})_4\text{M}$		Magnetic Moment	ΔE [Quartet–Doublet]	(kcal/mol)
	Expt ⁵	$\mu_{so} = \sqrt{4S(S+1)}$	B3PW91-D3/DZP	OPBE/DZP
V	1.82	1.73	35.6	31.0
Mn	3.78	3.87	–13.1	–15.3
Co	2.00	1.73	16.4	17.8
Cu	—	1.73	2.5	2.1

The energy differences between the triplet (quartet) and singlet (doublet) $(\text{nor})_4\text{M}$ structures calculated by the two different DFT methods are reasonably consistent. An exception is $(\text{nor})_4\text{Cr}$ for which the two different DFT methods predict very different

energy gaps, namely -42.0 kcal/mol (B3PW91-D3) or -19.0 kcal/mol (OPBE). This is because the B3PW91-D3 method can predict the closed shell singlet structure as the minimum, whereas the OPBE method predicts an open shell singlet structure. The closed shell singlet structure was not optimized successfully owing to the convergence problem.

In order to confirm further the energy gap between the closed shell singlet state and the triplet state for $(nor)_4Cr$, the very recently developed DLPNO-CCSD(T) method with def2-SPV basis sets implemented in the ORCA4 program^{36,37} was used to calculate the single point energies from geometries of the B3PW91-D3/DZP optimizations for $(CH_3)_4Cr$ as a simplified molecular model. Thus for $(CH_3)_4Cr$, the DLPNO-CCSD(T)/def2-SPV method predicts a triplet–singlet energy gap of -43.4 kcal/mol which is close to those of -43.8 and -44.5 kcal/mol calculated by the B3PW91-D3/DZP and OPBE/DZP methods, respectively. The agreement of the calculated triplet–singlet energy gaps of ~ 44 kcal/mol for $(CH_3)_4Cr$ using the relatively expensive DLPNO-CCSD(T)/def2-SPV method with those obtained from the less expensive B3PW91-D3/DZP and OPBE/DZP methods suggests that the singlet-triplet energy gap of -42.0 kcal/mol obtained by the B3PW91-D3/DZP method for $(nor)_4Cr$ is close to the true value. The calculated magnetic moments are remarkably consistent with the experimental magnetic data⁵ (Tables 1 and 2). Thus both theoretical methods predict high spin states for the d^2 and d^3 complexes $(nor)_4Cr$ and $(nor)_4Mn$, but low spin states for $(nor)_4Fe$ and $(nor)_4Co$.

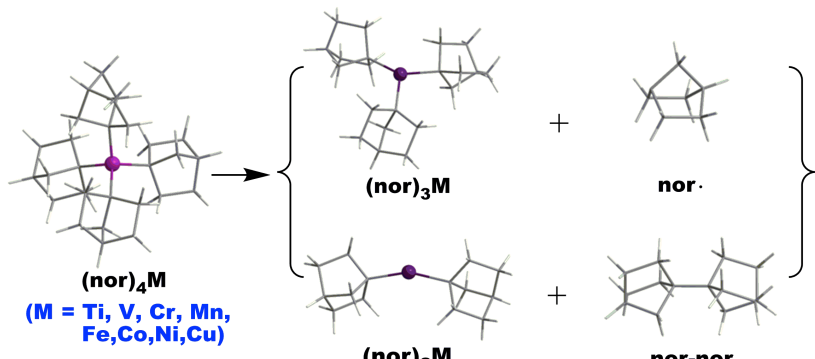


Figure 3. The two dissociation schemes of the $(nor)_4M$ structures

The dissociation energies (kcal/mol) for the reactions $(nor)_4M \rightleftharpoons (nor)_3M + nor\cdot$ (Figure 3 and Table 3) and $(nor)_4M \rightleftharpoons (nor)_2M + nor-nor$ (Figure 3 and Table 4) have been computed by the B3PW91 method with and without the dispersion correction. *The results indicate that dispersion effects play an important role in determining the dissociation energy.* Thus the dispersion effect is found to stabilize the $(nor)_4M$ derivatives by ~ 21 kcal/mol or the $(nor)_3M$ by ~ 25 kcal/mol. For comparison, the dissociation energies were also calculated by the OPBE method. However, the OPBE

method also consistently underestimates the dissociation energies compared with results calculated by the B3WP91-D3 method including the dispersion correction.

The dissociation energies for the reactions $(\text{nor})_4\text{M} \rightarrow (\text{nor})_3\text{M} + \text{nor}\cdot$ (Figure 3 and Table 3) calculated by the B3WP91-D3 method suggest that all of the $(\text{nor})_4\text{M}$ structures are strongly favored energetically towards dissociation of one of the four norbornyl groups. The titanium derivative $(\text{nor})_4\text{Ti}$ is the most favored with a dissociation energy of 77.1 kcal/mol, whereas $(\text{nor})_4\text{Cu}$ is the least favored with a dissociation energy of only 13.6 kcal/mol. Although the B3WP91 and the OPBE methods not considering dispersion both predict energetically favored $(\text{nor})_4\text{M}$ towards $(\text{nor})_4\text{M} \rightarrow (\text{nor})_3\text{M} + \text{nor}\cdot$ dissociation except for the copper derivative, they underestimate the dissociation energy by ~20 kcal/mol with respect to this energy difference. If dispersion is not considered, dissociation of the copper complex $(\text{nor})_4\text{Cu}$ becomes exothermic, liberating -5.8 kcal/mol (B3WP91) or -13.9 kcal/mol (OPBE).

Table 3. Dissociation energies for the reactions $(\text{nor})_4\text{M} \rightarrow (\text{nor})_3\text{M} + \text{nor}\cdot$ (kcal/mol).

$(\text{nor})_4\text{M} \rightarrow (\text{nor})_3\text{M} + \text{nor}\cdot$				
	B3PW91-D3	B3PW91 ^a	$\Delta E(-\text{D3})^b$	OPBE
Ti	77.1	56.9	20.2	54.1
V	66.0	44.4	21.6	34.0
Cr	56.5	38.5	18.0	28.0
Mn	46.8	24.6	22.2	16.6
Fe	56.5	31.1	25.4	22.7
Co	45.5	23.0	22.5	17.5
Ni	37.2	17.6	19.6	8.9
Cu	13.6	-5.8	19.4	-13.9

^a The energies are computed as the single point energies from the geometries of B3PW91-D3 method.

^b $\Delta E(-\text{D3}) = E[(\text{B3PW91-D3}) - E(\text{B3PW91})]$

For the alternative dissociation pathway $(\text{nor})_4\text{M} \rightarrow (\text{nor})_2\text{M} + \text{nor-nor}$, liberating 1-norbornyl dimer (Figure 3 and Table 4), the predictions obtained by the B3WP91-D3 method with the dispersion correction suggest that only $(\text{nor})_4\text{Ti}$ and $(\text{nor})_4\text{V}$ are clearly viable with dissociation energies of 41.3 kcal/mol and 23.4 kcal/mol, respectively. The $(\text{nor})_4\text{Cr}$ and $(\text{nor})_4\text{Fe}$ derivatives are only marginally viable energetically towards nor-nor dissociation with nearly zero calculated dissociation energies of 3.4 kcal/mol and 4.9 kcal/mol, respectively. For the other first row transition metals, such as manganese, cobalt, nickel, and copper, the dissociation energies even with the dispersion correction suggest that their $(\text{nor})_4\text{M}$

complexes are disfavored towards dissociation of the coupled nor-nor ligand. This is consistent with the lower experimental thermal stabilities of the manganese and cobalt derivatives up to 100°C and the fact that the nickel and copper derivatives have not been synthesized.⁵ However, the calculations using the B3WP91 and OPBE methods without the dispersion effect find all of the (nor)₄M structures except for the titanium derivative to be disfavored towards (nor)₄M \rightarrow (nor)₂M + nor-nor dissociation. This indicates the major role played by the dispersion effect in stabilizing the (nor)₄M complexes. However, even though the (nor)₄M \rightarrow (nor)₂M + nor-nor dissociation process is energetically favorable for many of the metals, this process is likely to have a high activation barrier since it involves simultaneous rupture of two M–C bonds and joining the two resulting nor[•] fragments.

Table 4. Dissociation energies for the reactions (nor)₄M \rightarrow (nor)₂M + nor-nor (kcal/mol).

	(nor) ₄ M \rightarrow (nor) ₂ M+nor-nor			
	B3PW91-D3	B3PW91 ^a	$\Delta E(-D3)$ ^b	OPBE
Ti	41.3	18.6	22.7	14.6
V	23.4	-2.5	25.9	-10.9
Cr	3.4	-16.9	20.3	-25.2
Mn	-3.6	-41.1	27.5	-43.7
Fe	4.9	-22.7	27.6	-24.2
Co	-9.3	-36.8	27.5	-39.4
Ni	-25.2	-49.6	24.4	-58.6
Cu	-48.4	-72.8	24.4	-79.2

^a The energies are computed as the single point energies from the geometries of B3PW91-D3 method.

^b $\Delta E(-D3) = E[(B3PW91-D3) - E(B3PW91)]$

The dissociation energy of the 1-norbornyl dimer nor-nor into two free 1-norbornyl radicals nor[•] considering the dispersion effect is $D_e = 105.6$ (B3WP91-D3). This is consistent with the (nor)₄M \rightarrow (nor)₂M + nor[•] + nor[•] dissociation energies (Table 5) being ~ 106 kcal/mol higher than the (nor)₄M \rightarrow (nor)₂M + nor-nor dissociation energies (Table 4). This difference is nearly equal to the dissociation energy of the nor-nor molecule into two 1-norbornyl radicals nor[•]. Furthermore, the energy required for dissociation of the norbornyl radical from (nor)₄M by the process (nor)₄M \rightarrow (nor)₃M + nor[•] is comparable or higher than that for removing the norbornyl radical from (nor)₃M by the process (nor)₃M \rightarrow (nor)₂M + nor[•]. This means that disproportionation of (nor)₃M into (nor)₄M + (nor)₂M is thermoneutral or slightly exothermic. This is consistent with the experimentally

observed⁵ disproportionation of the metal halide starting materials with the metals in the +2 or +3 oxidation states upon reactions with 1-norbornyllithium to give (nor)₄M (M = Cr, Mn, Fe, Co), with the metal in the unusual +4 oxidation state.

The experimental structures for (nor)₄Fe and (nor)₄Co as determined by X-ray crystallography^{8,9} both have C_s symmetry (Figure 2). Using the experimental (nor)₄Fe and (nor)₄Co geometries as starting structures leads to final optimized structures which are saddle points rather than true minima since they have small imaginary vibrational frequencies (Tables 6 and 7). This may be a consequence of crystal lattice constraints retaining the symmetric C_s geometries of (nor)₄Fe and (nor)₄Co. The theoretical predictions for the Fe-C distances and C-Fe-C angles in (nor)₄Fe are consistent with the experimental results (Table 6). However, the deviations between the optimized Co-C distances and C-Co-C angles and those of the experimental (nor)₄Co structure determined by X-ray crystallography are somewhat larger. These discrepancies may relate to our theoretical studies assuming gas phase species whereas the experimental structures are obtained in the crystalline state. In addition, the disorder in the X-ray structural determinations may limit the accuracy of the experimentally determined geometric parameters.

Table 5. Other dissociation energies for the (nor)₄M and (nor)₃M derivatives.

	(nor) ₄ M \square (nor) ₂ M + nor [•] + nor [•]			
	B3PW91-D3	B3PW91 ^a	$\Delta E(-D3)$ ^b	OPBE
Ti	147.0	114.2	32.1	104.6
V	129.1	93.0	36.8	79.2
Cr	109.0	78.7	30.3	64.9
Mn	92.0	54.5	37.5	46.4
Fe	110.6	72.9	37.7	65.8
Co	96.3	58.7	37.6	50.6
Ni	80.4	46.0	34.4	31.4
Cu	57.2	22.8	34.5	10.8
	(nor) ₃ M \square (nor) ₂ M + nor [•]			
	B3PW91-D3	B3PW91 ^a	$\Delta E(-D3)$ ^b	OPBE
Ti	69.8	57.3	12.5	50.5
V	63.1	48.7	14.4	45.2
Cr	52.5	40.1	12.4	36.9
Mn	45.2	29.9	15.3	29.8
Fe	54.0	41.8	12.2	43.1
Co	50.8	35.7	15.0	33.1
Ni	43.3	28.4	14.8	22.6
Cu	43.7	28.5	15.1	24.7

^a The energies are computed as the single point energies from the geometries of B3PW91-D3 method.

$$^b \Delta E(-D3) = E[(B3PW91-D3) - E(B3PW91)]$$

The optimized $(nor)_4M$ structures indicate that $(nor)_4Ti$ has the largest average metal–carbon distance of 2.075 Å (B3WP91-D3) or 2.143 Å (OPBE), and that $(nor)_4Fe$ has the shortest metal–carbon distance of 1.915 Å (B3WP91-D3) or 1.971 Å (OPBE). Surprisingly, this disagrees with the experimental results indicating a Co-C bond distance of 1.920 Å in $(nor)_4Co$ is shorter than the Fe-C bond of 1.993 Å (Table 8).

Table 6. Comparison of the calculated M–C distances (Å) and C–M–C angles of the $(nor)_4Fe$ structure with the experimentally determined C_s structure using X-ray crystallography. The numbers in parentheses are imaginary vibrational frequencies calculated for $(nor)_4Fe$ by the indicated theoretical methods.

$(nor)_4Fe$	Exp ⁸	OPBE (TS-44 <i>i</i>)	B3PW91-D3 (TS-56 <i>i</i>)
Fe-C2	2.002	1.977	1.919
Fe-C1	1.984	2.010	1.953
Fe-C4	2.002	1.964	1.914
C4-Fe-C1	109.4°	110.3°	110.3°
C2-Fe-C1	109.7°	109.9°	109.9°

Table 7. Comparison of the calculated M–C distances (Å) and C–M–C angles of the $(nor)_4Co$ structure with the experimentally characterized C_s symmetrical structure. The numbers in parentheses are imaginary frequencies calculated for $(nor)_4Co$ by the indicated theoretical methods.

$(nor)_4Co$	Exp ⁹	OPBE (78 <i>i</i> , 29 <i>i</i>)	B3PW91-D3 (83 <i>i</i> , 43 <i>i</i> , 31 <i>i</i>)
Co-C2	1.930(1.910)	1.961	1.924
Co-C4	1.928(1.911)	1.970	1.917
Co-C1	1.912(1.930)	2.082	2.005
C2-Co-C4	114.4° (113.4°)	106.9°	102.4°
C2-Co-C1	106.5° (106.9°)	107.6°	107.0°
C4-Co-C1	108.6° (109.0°)	107.1°	107.9°
C1-Co-C3	112.7° (111.6°)	122.1°	124.4°

*unconstrained refinement (constrained refinement)

Table 8. The average metal–carbon distances (Å) of the $(nor)_4M$ structures without symmetry constraints.

M	Ti	V	Cr	Mn	Fe	Co	Ni	Cu	
av. M-C (C_1)	B3PW91-D3	2.075	2.041	2.005	2.024	1.915	1.949	1.953	2.027
	OPBE	2.143	2.092	2.071	2.096	1.971	2.005	2.021	2.110
Exp. (C_s)						1.998	1.920		

(ref. 8) (ref. 9)

4. Summary

The theoretical dissociation energies of the reactions $(\text{nor})_4\text{M} \rightleftharpoons (\text{nor})_3\text{M} + \text{nor}^\bullet$ (kcal/mol) and $(\text{nor})_4\text{M} \rightleftharpoons (\text{nor})_2\text{M} + \text{nor-nor}$ indicate that dispersion effects play a significant role in stabilizing the $(\text{nor})_4\text{M}$ compounds (M = Ti to Cu). Thus all of these $(\text{nor})_4\text{M}$ (M = Ti to Cu) derivatives are viable with respect to 1-norbornyl radical dissociation when the dispersion effect is considered. However, $(\text{nor})_4\text{Cu}$ becomes disfavored if the dispersion correction is ignored. Thus the stability of the $(\text{nor})_4\text{M}$ molecules is seen to arise from the favorable combination of steric and dispersion force effects of the four 1-norbornyl groups tetrahedrally disposed around the metal atom and maximizing the dispersion attraction between them. The tri-1-norbornyl derivatives $(\text{nor})_3\text{M}$ appear to be disfavored with respect to disproportionation into $(\text{nor})_4\text{M} + (\text{nor})_2\text{M}$. This is consistent with the experimental syntheses of the $(\text{nor})_4\text{M}$ (M = Cr to Co) derivatives with the metal in the +4 oxidation by reactions with 1-norbornyllithium with metal halides in the +2 or +3 metal oxidation states. Both the OPBE method and the BPW91 method predict high spin states for the d^2 and d^3 complexes $(\text{nor})_4\text{Cr}$ and $(\text{nor})_4\text{Mn}$ but low spin states for $(\text{nor})_4\text{Fe}$ and $(\text{nor})_4\text{Co}$, consistent with experiment.

Acknowledgments. The research in Chengdu was supported by the Sichuan Provincial Foundation for Distinguished Young Leaders of Disciplines in Science and Technology of China (Grants 2019JDJQ0051 and 2019JDJQ0050), the National Natural Science Foundation for Young Scientists of China (Grant No. 11605143), the Open Research Subject of the Key Laboratory of Advanced Computation in Xihua University (Grant No szjj2017-011 and szjj2017-012), the Young Scholarship Plan of Xihua University (Grant 0220170201), and the Chunhui Program of the Ministry of Education of China (Grant Z2017091). The research in Georgia was supported by the U. S. National Science Foundation, Grant CHE-1661604.

The authors declare no competing financial interests.

Supporting Information. Table S1 to Table S16: Atomic coordinates of the optimized structures for the $(\text{nor})_4\text{M}$ (M = Ti, V, Cr, Mn, Fe, Co, Ni, Cu) complexes; Complete Gaussian09 reference (Reference 35).

References

- (1) Rasmussen, S. C., The 18-electron rule and electron counting in transition metal compounds: theory and application. *Chem. Texts* **2015**, *1*, 10.
- (2) Tolman, C. A. The 16 and 18 electron rule in organometallic chemistry and homogenous catalysis. *Chem. Soc. Rev.* **1972**, *1*, 337-353.
- (3) Craig, D. P.; Doggett, G. Theoretical basis of the “rare-gas rule”. *J. Chem. Soc.* **1963**, 4189-4198.
- (4) Bredt, J. Über sterische Hinderung in Brückenringen (Bredtsche Regel) und über die *meso-trans*-Stellung in kondensierten Ringsystemen des Hexamethylens. *Liebigs Ann. Chem.* **1924**, *437*, 1–13.
- (5) Bower, B. K.; Tennent, H. K. Transition metal bicyclo[2.2.1]hept-1-yls. *J. Am. Chem. Soc.* **1972**, *94*, 2512–2513
- (6) Jacob, K.; Thiele, K.-H. Zur Existenz von 1-Norbornylverbindungen des Wolframs und Molybdäns. *Z. anorg. Allg. Chem.* **1984**, *508*, 50–54.
- (7) Kolodziej, R. M.; Schrock, R. R.; Davis, W. M. Synthesis and characterization of Mo(nor)₄ (nor = 1-norbornyl). *Inorg. Chem.* **1988**, *27*, 3253–3255.
- (8) Lewis, R. A.; Smiles, D. E.; Darmon, J. M.; Stieber, S. C. E.; Wu, G.; Hayton, T. W. Reactivity and Mössbauer spectroscopic characterization of an Fe(IV) ketimide complex and reinvestigation of an Fe(IV) norbornyl complex. *Inorg. Chem.* **2013**, *52*, 8218–8227.
- (9) Byrne, E. K.; Richeson, D. S.; Theopold, K. H. Tetrakis(1-norbornyl)cobalt, a low spin tetrahedral complex of a first row transition metal. *Chem. Commun.* **1986**, 1491–1492.
- (10) Dimitrov, V.; Linden, A. A pseudodetrahedral, high-oxidation state organonickel compound: synthesis and structure of bromotris(1-norbornyl)-nickel(IV). *Angew. Chem. Int. Ed.* **2003**, *42*, 2631-2633.
- (11) Lehmkuhl, H.; Dimitrov, V. \square^2 -Alkin-Komplexe des \square^5 -Cyclopenta-dienylnickel-1-norbornyls. *J. Organometal. Chem.* **1996**, *519*, 69–73.
- (12) Wagner J. P; Schreiner, P. R. London dispersion decisively contributes to the thermodynamic stability of bulky NHC-coordinated main group compounds, *J. Chem. Theory Comput.* **2016**, *12*, 231–237.
- (13) Liptrot D. J. ; Power P. P. London dispersion forces in sterically crowded inorganic and organometallic molecules, *Nat. Rev. Chem.* **2017**, *1*, 0004.
- (14) Israelachvilli, J. N. *Intermolecular and Surface Forces*; 3 ed., Academic Press: Waltham, USA, **2011**.
- (15) Liptrot D. J. ; Power P. P. London dispersion forces in sterically crowded inorganic and organometallic molecules, *Nat. Rev. Chem.* **2017**, *1*, 0004(.

(16) Schreiner, P. R.; Chernish, L. V.; Gunchenko, P. A.; Tikhonchuk, E. Y.; Hausmann, H.; Serafin, M.; Schlecht, S.; Dahl, J. E. P.; Carlson, R. M. K.; Fokin, A. A. Overcoming lability of extremely long alkane carbon–carbon bonds through dispersion forces, *Nature* **2011**, *477*, 308–310

(17) Rösel, S.; Becker, J.; Allen, W. D.; Schreiner, P. R. Probing the delicate balance between Pauli repulsion and London dispersion with triphenylmethyl derivatives, *J. Am. Chem. Soc.* **2018**, *140*, 14421–14432

(18) Wagner, J. P.; Schreiner, P. R. London dispersion in molecular chemistry—reconsidering steric effects, *Angew. Chem. Int. Ed.* **2015**, *54*, 12274–12296.

(19) Casitas, A.; Rees, J. A.; Goddard, R.; Bill, E.; DeBeer, S.; Fürstner, A. Two exceptional homoleptic iron(IV) tetraalkyl complexes. *Angew. Chem. Int. Ed.* **2017**, *56*, 10108–10113.

(20) Liptrot, D. J.; Guo, J.-D.; Nagase, S.; Power, P. P. Dispersion forces, disproportionation, and stable high-valent transition metal alkyls. *Angew. Chem. Int. Ed.* **2016**, *55*, 14766–14769.

(21) Dunning Jr., T. H. Gaussian basis functions for use in molecular calculations. I. Contraction of (9s5p) atomic basis sets for the first-row atoms. *J. Chem. Phys.* **1970**, *53*, 2823–2833.

(22) Huzinaga, S. Gaussian-type functions for polyatomic systems. I. *J. Chem. Phys.* **1965**, *42*, 1293–1302.

(23) Wachters, A. J. H. Gaussian basis set for molecular wavefunctions containing third-row atoms. *J. Chem. Phys.* **1970**, *52*, 1033–1036.

(24) Hood, D. M.; Pitzer, R. M.; Schaefer, H. F. Electronic structure of homoleptic transition metal hydrides: TiH_4 , VH_4 , CrH_4 , MnH_4 , FeH_4 , CoH_4 , and NiH_4 . *J. Chem. Phys.* **1979**, *71*, 705–712.

(25) Becke, A. D. Density-functional exchange-energy approximation with correct asymptotic-behavior, *Phys. Rev. A*, **1988**, *38*, 3098–3100.

(26) Perdew, J. P.; Wang, Y. Accurate and simple analytic representation of the electron gas correlation energy, *Phys. Rev. B*, **1992**, *45*, 13244–13249.

(27) Perdew, J. P.; Burke, K.; Wang, Y. Generalized gradient approximation for the exchange-correlation hole of a many-electron system. *Phys. Rev. B*, **1996**, *54*, 16533–16539.

(28) Dierksen, M.; Grimme, S. An efficient approach for the calculation of Franck-Condon integrals of large molecules. *J. Chem. Phys.* **2005**, *122*, 244101.

(29) Grimme, S. Density functional theory with London dispersion corrections. *Sires Comput. Mol. Sci.* **2011**, *1*, 211–228.

- (30) Handy, N. C.; Cohen, A. J. Left-right correlation energy. *Mol. Phys.*, **2001**, *99*, 403–412.
- (31) Boese, A. D.; Handy, N. C. A new parametrization of exchange-correlation generalized gradient approximation functionals. *J. Chem. Phys.*, **2001**, *114*, 5497–5503.
- (32) Hoe, W.-M.; Cohen, A.; Handy, N. C. Assessment of a new local exchange functional OPTX. *Chem. Phys. Lett.*, **2001**, *341*, 319–328.
- (33) Perdew, J. P.; Burke, K.; Ernzerhof, M. Generalized gradient approximation made simple. *Phys. Rev. Lett.*, **1996**, *77*, 3865–3868.
- (34) Swart, M.; Gruden, M. Spinning around in transition metal chemistry. *Acc. Chem. Res.* **2016**, *49*, 2690–2697.
- (35) Frisch, M. J.; Trucks, G. W.; Schlegel, H. B.; Scuseria, G. E.; Robb, M. A.; Cheeseman, J. R.; Scalmani, G.; Barone, V.; Mennucci, B.; Petersson, G. A.; et al. Gaussian 09, Revision A.02; Gaussian, Inc., Wallingford CT, **2009**.
- (36) Neese, F.; Atanasov, M.; Bistoni, G.; Maganas, D.; Ye, S. Chemistry and quantum mechanics in 2019: Give us insight and numbers. *J. Am. Chem. Soc.* **2019**, *141*, 2814–2824.
- (37) Guo, Y.; Ripplinger, C.; Becker, U.; Liakos, D. G.; Minenkov, Y.; Cavallo, L.; Neese, F. An improved linear scaling perturbative triples correction for the domain based local pair-natural orbital based singles and doubles coupled cluster method [DLPNO-CCSD(T)]. *J. Chem. Phys.* **2018**, *148*, 011101.

For the Table of Contents

Dispersion Effects in Stabilizing Organometallic Compounds: The Tetra-1-norbornyl Derivatives of the First Row Transition Metals as Exceptional Examples

Huidong Li,^{*} Yucheng Hu,^a Di Wan,^a Ze Zhang,^a Qunchao Fan,^a R. Bruce King^{b*}, and Henry F. Schaefer III^b

The theoretical energies for the dissociation of 1-norbornyl (nor) ligands from (nor)₄M (M = Ti to Cu) through the reactions (nor)₄M \rightarrow (nor)₃M + nor• and (nor)₄M \rightarrow (nor)₂M + nor-nor indicate that dispersion effects play a major role in determining the exceptional stability of the (nor)₄M (M = Ti to Co) derivatives.

